check for updates

Effect of inulin and xanthan gum on the properties of 3D printed Tartary buckwheat paste

Yaojia Li[1,2]

Mantihal Sylvester[3]

Ai Ling Ho[3]

Jau-Shya Lee[1+]

[1]*Food Safety and Security Research Group, Faculty of Food Science and Nutrition, Universiti Malaysia Sabah, 88400 Kota Kinabalu, Sabah, Malaysia.*
[1]*Email: jslee@ums.edu.my*
[1,2]*Email: liyaojia910@sina.com*
[2]*Faculty of Agricultural Science, Panxi Crops Research and Utilization Key Laboratory, Xichang University, 615000 Xi Chang, Sichuan, China.*
[3]*Functional Food Research Group, Faculty of Food Science and Nutrition, Universiti Malaysia Sabah, 88400 Kota Kinabalu, Sabah, Malaysia.*
[3]*Email: s.mantihal@ums.edu.my*
[3]*Email: alho@ums.edu.my*

(+ Corresponding author)

ABSTRACT

This work aimed to investigate the effect of inulin and XG on the 3D printability of Tartary buckwheat paste. A 2×3 factor design comprising three levels of inulin (6%, 10%, and 14%) and three levels of xanthan gum (XG) (0.4%, 0.8%, and 1.2%) was used. The effect of inulin and XG on the rheological properties (yield stress, flow behaviour, viscoelasticity, and creep-recovery property), 3D printed structure, and microstructure properties of Tartary buckwheat paste were investigated. Compared with the control sample, a high amount of XG (0.4% and 1.2%) shifted the ink to a more solid-like form and improved the consistency (K), mechanical strength (yield stress, storage modulus (G')), resistance to deformation, and recoverability, while a high amount of inulin (14%) weakened these properties. Scanning electron microscopy (SEM) revealed that adding XG (0.4% and 1.2%) in the ink with 6% and 10% of inulin reinforced the ink structure. This study also identified the best combination of XG and inulin to facilitate the printing of Tartary buckwheat paste and produce a final product with an exquisite appearance. This study provided more insights for developing 3D printing of Tartary buckwheat foods rich in inulin.

Contribution/Originality: This study was the first to incorporate inulin and xanthan gum into Tartary buckwheat pastes for 3D printing and obtain a delicate 3D printed product. The results would contribute to a better understanding of the role of inulin and xanthan gum in Tartary buckwheat paste and provide references for the development of 3D printed Tartary buckwheat paste products.

1. INTRODUCTION

Three-dimensional (3D) printing is an innovative process technology that combines 3D model design and production to build complex structures layer by layer (Jiménez, Romero, Domínguez, Espinosa, & Domínguez, 2019). This technology can produce complex geometries and high-quality products without using labour-intensive machines and expensive models, realise personalisation and digitalisation of nutrition, simplify the food supply chain, and enable economical processing with less waste (Godoi, Prakash, & Bhandari, 2016). Due to these benefits, 3D food printing as a promising technique has attracted considerable attention. Tartary buckwheat (Fagopyrum tataricum (L.) Gaertn) is a gluten-free grain cultivated in large abundance in the mountains of southwestern China. It was mostly consumed

as noodles, steamed bread, and cakes, or used to make other local snacks like caramel treats. It is reported to contain a high flavonoid content (9.12 mg/g dry weight (DW)), especially rutin content (13.99 g/kg DW), which is much higher than that of common buckwheat flour (0.15 g/kg DW) (Sinkovič, Deželak, & Meglič, 2022; Sinkovič, Sinkovič, & Meglič, 2021). It has been shown that flavonoids lower the amounts of C-peptide, glucagon, triglycerides, and blood urea nitrogen in rats and mice with type 2 diabetes (Yao et al., 2008; Zhang, Yao, Wang, & Ren, 2011). It can also inhibit the activity of the angiotensin-I converting enzyme (ACE) to prevent hypertension (Tsai, Deng, Tsai, & Hsu, 2012). These health benefits have attracted attention in recent years, leading to the development of various food products using Tartary buckwheat flour.

Inulin is a natural polysaccharide mainly extracted from chicory roots for industrial use. Native chicory inulin is a mixture of short and long polymer chains with degrees of polymerisation (DP) ranging from 2 to 60 (Kou et al., 2018). Short (DP from 2 to 7) or long chain (DP ≥ 23) inulin can be extracted from natural inulin in industry to obtain commercial products (Roberfroid, 2004). As a fraction of dietary fibre, it has a prebiotic function, which is able to prevent and relieve constipation via the regulation of gut microbiota, reduce the risk of gastrointestinal diseases, and also ameliorate blood sugar and promote mineral absorption (Coxam, 2005; Shoaib et al., 2016). Apart from health benefits, it can be utilised as a structure-forming agent, a low-calorie sweetener, and a fat replacer, thereby improving the rheological properties of products, increasing flavours, and controlling water retention in products (Luo et al., 2017; Tárrega, Torres, & Costell, 2011). A number of authors have combined inulin with starch or hydrocolloids, which can work with these other ingredients to create stronger effects (Ji et al., 2021; Mieszkowska & Marzec, 2016; Torres, Tárrega, & Costell, 2010; Witczak, Witczak, & Ziobro, 2014). Xanthan Gum (XG) is an extracellular polysaccharide secreted by microorganisms and industrially produced by fermentation (Imeson, 2010a). It has good water-holding, thickening, and gelling properties and can be added to food products to obtain the desired qualities. In the study by Kim et al. (2019), the incorporation of 0.5 g/100 g XG in cookie dough was reflected in increased shear modulus and extrudability to get good 3D printability. Similarly, adding XG to rice dough has improved viscosity and elastic modulus (Demirkesen, Mert, Sumnu, & Sahin, 2010). Because of the adverse effects of refined foods in the daily diet, there is a growing trend to add natural fibre to food products. Inulin is one of the most commonly used diet fibre in food systems. Likewise, Tartary buckwheat also possesses high nutritional value and offers health benefits. Hence, using 3D printing technology to develop Tartary buckwheat products that are rich in dietary fibre and have an exquisite appearance can increase individuals' choices concerning nutritious diets and customise nutritious foods. However, because Tartary buckwheat flour is gluten-free, it lacks the strength and elasticity needed for 3D printed foods. As a result, hydrocolloids must be added to the ink formulation in order to improve the ink's 3D printability. Therefore, this study investigated the 3D printability of Tartary buckwheat paste by adding inulin and XG. The effect of inulin and XG on the rheological properties (yield stress, flow behaviour, viscoelasticity, and creep-recovery properties), 3D printed structure, and microstructure properties of Tartary buckwheat paste were investigated. This study provided more insights into the development of 3D printed inulin rich Tartary buckwheat foods.

2. MATERIALS AND METHODS

2.1. Materials

The material used for printing ink preparation consisted of inulin (COSUCRA-FIBRULINE™, Belgium) with DP in the range of 2-60 with 93.1% inulin and 6.8% oligosaccharide and xanthan gum (Weifeng biological Co., Ltd., Zhengzhou, China). Tartary buckwheat puffed flour with 10.6 g/100g protein and 65.5 g/100g carbohydrate (Hangfei Tartary Buckwheat Technology Development Co., Ltd., Sichuan, China), trehalose (Huaxi Biological Co., Ltd., Guangzhou, China), and milk (Yili, Co., Ltd., Mongolia, China) were used.

2.2. Printing Ink Preparation

Different amounts of XG, inulin, 4% trehalose, and 16% Tartar buckwheat flour (based on the amount of milk used) were added to 40 g of milk and mixed thoroughly. The mixture was kept in a water bath at 70 ± 0.2 °C for 30 min and then left for 30 minutes to cool down to room temperature. The remaining 10 g of milk was added to the cooled Tartary buckwheat paste and stirred with a scraper for three minutes until it homogenised. It would be used for 3D printing. The percentage of inulin and XG used in the ink is presented in Table 1.

Table 1. The percentage (%)* of independent variables used in the ink formulations.

Sample	Inulin/%	XG/%
Control	0	0
6I04X	6	0.4
6I08X	6	0.8
6I12X	6	1.2
10I04X	10	0.4
10I08X	10	0.8
10I12X	10	1.2
14I04X	14	0.4
14I08X	14	0.8
14I12X	14	1.2

Note: *The percentage was based on the amount of milk used.

2.3. 3D Printing

The sample was printed with an extrusion-type 3D food printer (Shiyin Tech. Co. Ltd., Hangzhou, China). A cuboid (25 mm length, 25 mm width, and 10 mm height) was designed using computer-aided design (CAD) software to evaluate the differences in 3D-printed structures. The printing parameters were as follows: printing temperature of 25 °C, printing nozzle size of 0.84 mm, printing speed of 30 mm/s, infill density of 100%, rectilinear infill pattern, initial layer thickness of 0.6 mm, and nozzle height of 2.0 mm.

2.4. Rheological Properties

Rheological measurements were conducted using a rotational rheometer (AR2000ex, TA Instruments, America) based on a 40-mm parallel plate with a gap of 1000 μm (Xing et al., 2022). Flow sweeps were conducted at shear rates of 0.1 to 100 (1/s) to measure the change in viscosity of materials with an increase in shear rate. Yield performance was tested in the 1-1000 Pa range at an oscillation frequency of 1 Hz. Amplitude sweeps were performed at a constant frequency of 1 Hz over an amplitude range of 0.01-100% to determine the region of the linear viscoelastic range. A frequency sweep analysis (range of 0.1 to 10 Hz at a constant deformation strain of 0.1%) was used to record the change of G', G'', and $\tan\delta$ (G''/G') with frequency. Flow behaviour experimental data were described by a power law model as Equation 1.

$$\tau = K \times \gamma^n \qquad (1)$$

Where τ is the shear stress (Pa), K is the consistency coefficient (Pa·s^n), γ is shear rate (s^{-1}), and n is the flow behaviour index. A previous study recommended creep-recovery tests (Xing et al., 2022). The test was carried out in the linear viscoelastic region at a constant stress of 10 Pa for 180 s, with a recovery time of 420 s after removal of the applied stress. The experimental data were fitted by Burger's model as Equations 2 and 3 (Brito-Oliveira, Moraes, Pinho, & Campanella, 2022).

$$J(t) = J_0 + \frac{t}{\eta_0} + J_1 \times (1 - exp^{-t/\lambda_{ret}}) \text{ for } t < t_1 \qquad (2)$$

$$J(t) = \frac{t_1}{\eta_0} - J_1 \times (1 - exp^{t_1/\lambda_{ret}}) \times exp^{-t/\lambda_{ret}} \text{ for } t > t_1 \qquad (3)$$

Where J is a compliance (Pa^{-1}), J_0 is an instantaneous compliance, J_1 is a retardation compliance (Pa^{-1}), η_0 is zero shear viscosity (Pa·s), λ_{ret} is a retardation time (s), and t_1 is a time after which the stress was removed (s).

Equation 4 provided by Pulatsu, Su, Lin, and Lin (2020), quantified the recovery (R_e) in order to assess the ink's capacity for recovery after stress removal .

$$R_e = \frac{R_m - R_f}{R_f} \tag{4}$$

Where R_m and R_f are the maximum and final strain (%) values, respectively.

The test temperature of 25 °C was equal to the printing temperature. To avoid evaporation, silicone oil was added to the edges of the samples before the test. All the tests were repeated three times, and the averages were used to plot the curves.

2.5. Scanning Electron Microscopy

Printing inks were first dried in a freeze-dryer and prepared into a powder. Dry samples were mounted on round base bars with double-sided tape and sputter-plated with gold (10 mA for 40 s). A scanning electron microscope (TEM300, Hitachi, Japanese) was used to observe the microstructure of the freeze-dried buckwheat paste at 2000 × magnification with an accelerating voltage of 5.0 kV.

2.6. Statistical Analysis

Analysis was performed in triplicate, and the recorded data were given as mean ± standard deviation. SPSS 23.0 was used to conduct analysis of variance (ANOVA), Tukey's test ($P \leq 0.05$), and two-way ANOVA to investigate whether there were significant differences among the data points and interaction effects among factors. Origin 9.0 was used to plot graphs and perform regression analysis.

3. RESULTS AND DISCUSSION

3.1. Rheology Behaviour

3.1.1. Yield Stress

Yield stress is the minimum force required to initiate flow and reflects the mechanical strength of the ink, which is related to print extrusion performance and the ability to hold printed shapes (Liu, Liang, Saeed, Lan, & Qin, 2019; Liu, Bhandari, & Zhang, 2020). A Two-factor ANOVA showed that XG, inulin, and their interactions significantly affected this parameter ($P < 0.05$). As seen in Figure 1, adding 0.4 % of XG did not significantly change the yield stress ($P > 0.05$), except for 14I04X, which had a lower ($P < 0.05$) yield stress than the control sample. However, a higher amount of XG (0.8% and 1.2%) significantly increased ($P < 0.05$) the yield stress of the inks. A study by Xing et al. (2022) also showed that the increase in the percentage of XG from 0.6% to 0.9% increased the yield stress of black-fungus pastes from 115 to 166.5 Pa. The rigid molecular chain of XG makes the ink with a high amount of XG have a stronger structure. It also increases the connections between starch molecules, improving the ink's strength (Abdel-Aal et al., 2019; Rong et al., 2022; Shalviri, Liu, Abdekhodaie, & Wu, 2010).

The yield stress of the ink with 0.8% and 1.2 % of XG decreased ($P < 0.05$) with the increase of inulin (from 6% to 14%) (Figure 1). Comparatively, the decreasing magnitude of yield stress was more significant with 14% of inulin than with 6% and 10% of inulin ($P < 0.05$). It suggests that inulin diluted the system, especially when the inks required higher forces to initiate flow. However, Guggisberg, Cuthbert-Steven, Piccinali, Bütikofer, and Eberhard (2009) found that long-chained inulin of high purity (DP > 23, purity: 99.5%) increased the yield stress of skimmed milk. Chiavaro, Vittadini, and Corradini (2007) also suggested that long-chain molecules in inulin (DP > 22) interacted with each other to form a gel and increased the gel strength of the material. The contradictory observations are probably related to the inulin used in this study, a mixture with a wide distribution of chain lengths (DP from 2 to 60). Low DP inulin makes it difficult to form gels and mainly acts as a diluting substance (Chiavaro et al., 2007; De Gennaro, Birch, Parke, & Stancher, 2000). Also, inulin in this study contained 6.8% oligosaccharides, which might interfere with starch network formation and reduce yield stress (Chang, Lim, & Yoo, 2004).
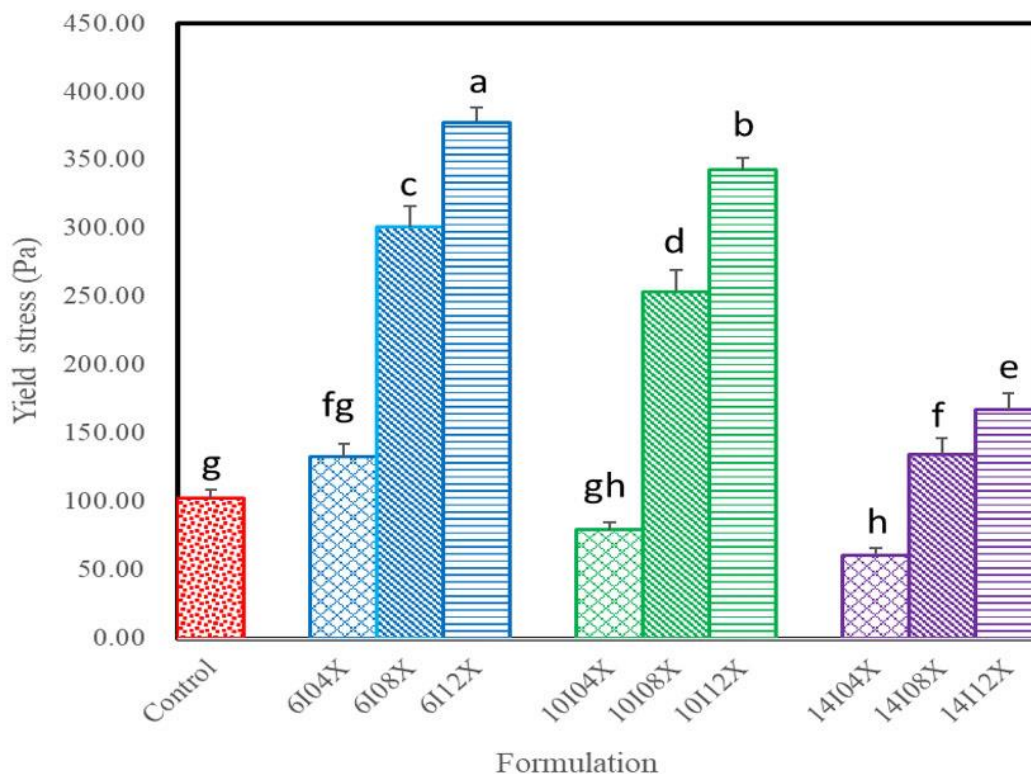
Figure 1. The yield stress values of each ink formulation. Each formulation was tested at 25°C and expressed as mean ± SD (n = 3).

Note: The different lowercase letters (a, b, c, d, e, f, g) in the histograms indicate-significant differences at a level of confidence of 0.05.

3.1.2. Flow Behaviour

In order to facilitate 3D printing, food material should have suitable flowability to be extruded through a fine nozzle (Godoi et al., 2016). The flow behaviour of the inks fitted the Power law model (R^2 > 0.95, Table 2). K is the consistency coefficient, reflecting the viscosity of the sample. n is the flow behavior index, with smaller n values indicating stronger shear thinning properties (Liu et al., 2019). A two-way ANOVA indicated that XG significantly affected K and n.

The interaction between inulin and XG also had a significant effect on these parameters ($P<0.05$), whereas inulin only had a significant effect on K values ($P>0.05$). All inks were observed to be non-Newtonian fluids with shear-thinning properties (n<1, Figure 2), which is essential for 3D printing (Liu et al., 2019). Incorporating 0.4% g of XG into inks significantly reduced the n value compared to the control, with further decreases at 1.2% of XG in inks with 6% and 10% of inulin ($P < 0.05$). Adding 0.8% and 1.2 % of XG also decreased the n value of inks with 14% of inulin ($P < 0.05$). Xing et al. (2022) observed that the n value of black-fungus pastes decreased from 0.31 to 0.26 when XG concentration increased from 0.3 to 0.6%.

The XG agglomerates formed by intermolecular forces at low shear rates are easily disrupted at high shear rates, thus increasing the shear-thinning behaviour of the ink (Imeson, 2010a). In contrast, the addition of inulin increased the n value, with the inks containing 10% and 14% of inulin (10I12X and 14I12X) having significantly higher ($P < 0.05$) n values than those with 6% of inulin (6I12X). Inulin forms a small crystalline network structure after shearing, which is not easily destroyed under shear stress (Imeson, 2010b). It indicates that XG increased the pseudoplasticity of the inks, but high amounts of inulin (10% and 14%) weakened this property.

Table 2. Power law model parameters of the flow curves of each ink formulation.

Formulation	Flow behaviour index (n)	Consistency coefficient (K, Pa·s^n)	R^2
Control	0.329 ± 0.008[a]	159.89 ± 9.59[g]	0.999
6I04X	0.298 ± 0.009[b]	210.58 ± 3.98[e]	0.998
6I08X	0.286 ± 0.005[bc]	241.39 ± 5.00[d]	0.996
6I12X	0.235 ± 0.011[d]	354.38 ± 6.37[a]	0.974
10I04X	0.291 ± 0.004[bc]	186.91 ± 5.47[f]	0.995
10I08X	0.298 ± 0.008[b]	232.77 ± 9.75[d]	0.996
10I12X	0.258 ± 0.007[c]	297.21 ± 2.36[b]	0.986
14I04X	0.304 ± 0.008[b]	156.41 ± 1.97[g]	0.999
14I08X	0.264 ± 0.008[c]	231.95 ± 3.64[d]	0.999
14I12X	0.269 ± 0.009[c]	266.60 ± 5.27[c]	0.994
Two-way ANOVA–p			
Factor I (Inulin)	0.058	< 0.001	
Factor II (XG)	< 0.001	< 0.001	
Factor I × Factor II	< 0.001	< 0.001	

Note: Each formulation was tested at 25 °C and expressed as mean ± SD (n = 3). The lowercase letters (a, b, c, d, e, f, g) in the same column indicate significant differences at a level of confidence of 0.05.
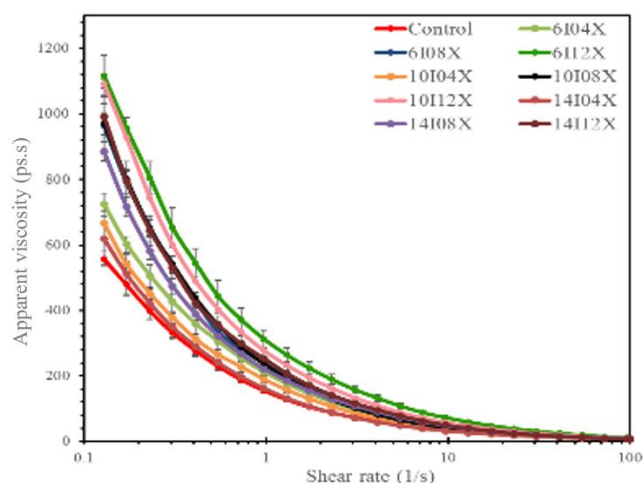

Figure 2. The apparent viscosity of each ink formulation.

The control sample and 14I04X showed the lowest K values (P > 0.05, Table 2). This value significantly increased (P < 0.05), with XG increasing from 0.4% to 1.2%. Demirkesen et al. (2010) also reported that adding XG increased the K value of rice dough. XG reduces water mobility in food through hydrogen bonds, thus increasing its viscosity (Xing et al., 2022). However, the K value significantly decreased (P < 0.05) when inulin was increased from 6% to 14% in inks with 0.4% and 1.2% of XG. This further confirms that the addition of inulin weakens the paste's structure. According to Witczak et al. (2014), adding highly soluble inulin (DP < 10 with 8% oligosaccharides) and granular inulin (DP ≥ 10 with 14% oligosaccharides) to potato starch pastes made them less sticky.

3.1.3. Viscoelasticity

Figure 3 shows the viscoelastic properties of the inks, with G′ defining the solid-like properties related to mechanical strength and G″ reflecting the liquid-like viscous characteristics. Inulin and XG significantly affect G′ and G″, but the interaction between them only significantly affects G′ (P < 0.05). Both G′ and G″ were frequency-dependent for all inks and exhibited solid-like properties (G′ > G″) (Liu, Zhang, Bhandari, & Wang, 2017). 10I04X and 14I04X inks had lower G' and G" than the control sample, but they were not significantly different (P > 0.05, Figure 3A and C). The addition of 0.8% and 1.2% of XG (6I08X, 6I12X, 10I08X, and 10I12X) resulted in significantly

higher G' and G" than the other samples (Figure 3B and D). The observations revealed that the structure-forming effect of XG enhances the mechanical strength and elasticity of the inks, but higher XG amounts (0.8% and 1.2%) also increase their liquid-like properties, which might relate to the increased consistency with the addition of XG. Conversely, the G' and G' of the inks showed a decreasing trend with the incorporation of inulin. For example, the G' and G" decreased in the order of 6I12X, 10I12X, 6I08X, 10I08X, 14I12X, and 14I08X (Figure 3B and D). As mentioned earlier, inulin weakens the gel strength of the ink. Similar results were found by Peressini and Sensidoni (2009), who found that the modulus of wheat dough was reduced by the addition of a mixture of inulin containing both long and short chains (DP: 2-60). G' and G" also went down when highly-soluble inulin (DP < 10, 8% oligosaccharides) and granular inulin (DP ≥ 10, 14% oligosaccharides) were added to maize-rice dough (Juszczak et al., 2012).
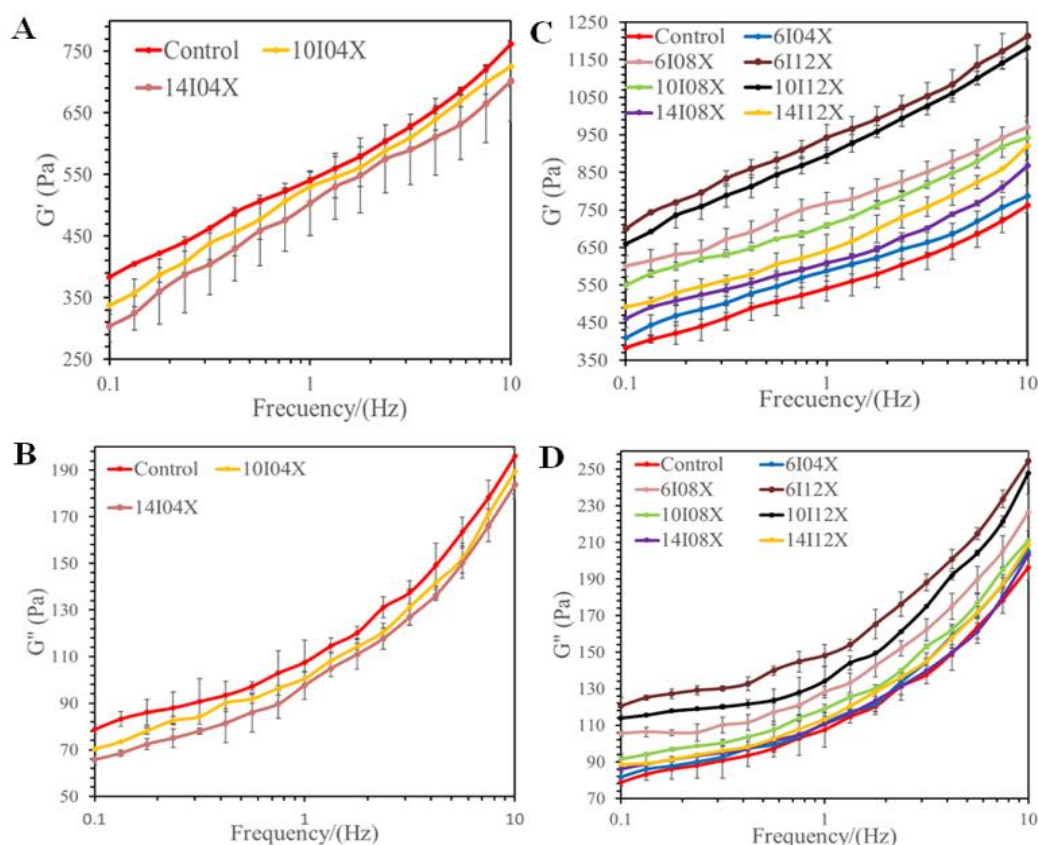
Figure 3. The dynamic rheological characteristics of each ink formulation. A and B storage modulus (G') while C and D Loss modulus (G"). Each formulation was tested at 25 ℃ and expressed as mean ± SD (n = 3).

The loss tangent (tan δ= G"/G') of the inks is shown in Figure 4, where a high tan δ value shows more viscous-like behaviour, and a low tan δ means more solid-like behaviour (Z Liu et al., 2017). XG, inulin and their interaction impact on this parameter were significant (P <0.05). As seen in Figure 4, Tan δ of all inks decreased first and then increased with increasing frequency, indicating that the inks had a more elastic nature at lower frequencies (<1 Hz) and more viscous properties at higher frequencies (>1 Hz). This demonstrated that the structure of the ink is unstable and easily destroyed at higher frequencies. A similar trend of tan δ with frequency was also observed in the rice paste and cookie dough (Liu, Bhandari, et al., 2020; Liu, Zhang, & Ye, 2020). Higher tan δ values were recorded in the control samples, 14I04X and 10I04X, with no significant difference (P>0.05), but a higher amount of XG (0.8% and 1.2%) significantly reduced the tan δ. The lowest tan δ values were observed in the inks with 1.2% of XG (6I12X and 10I12X), suggesting that XG shifted the inks towards solid-like properties with low fluidity. But inulin changed the inks' properties so that they behaved more like liquids. The tan δ of the inks with 14% inulin (14I04X, 14I08X, and

14I12X) was higher (P < 0.05) than that of the inks with 6% inulin (6I04X, 6I08X, and 6I12X).The corn-rice dough also gradually shifted to viscous properties with an increasing level of low-DP inulin (DP<10) (Juszczak et al., 2012).
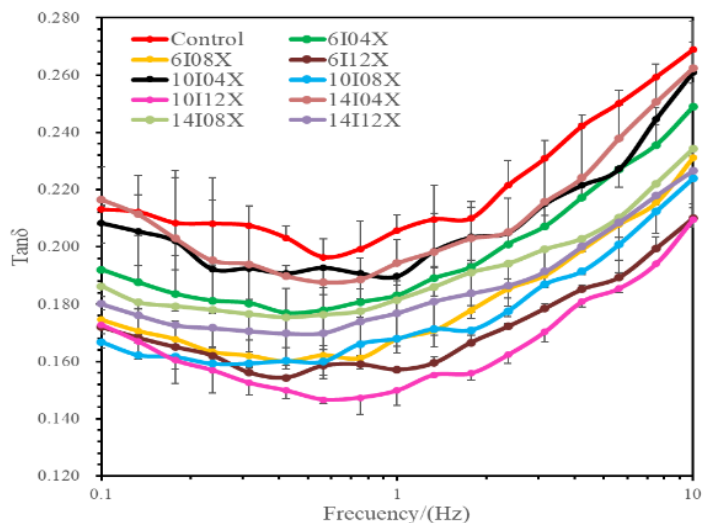
Figure 4. The loss tangent (Tan δ) of each ink formulation. Each formulation was tested at 25 ℃ and expressed as mean ± SD (n = 3).

3.1.4. Creep and Recovery Properties

In Figure 5, creep phase ($0 \leqslant t \leqslant 180$ s) indicates the Burger model. This model is made up of the Kelvin-Voigt model (a Hookean spring and a Newtonian dashpot placed parallel) and the Maxwell model (a Hookean spring and a Newtonian dashpot placed in series) that are put in series (Augusto, Ibarz, & Cristianini, 2013). When constant stress is applied, the material immediately experiences instantaneous deformation (J_0), which is the instantaneous response generated by the Hookean spring (Figure 5 (a)) in the Maxwell model. Then, the subsequent deformation is the superposition of the Newtonian dashpot deformation ($J_1 \times exp^{-t/\lambda_{ret}}$) and the retardation deformation (J_1) in the Kelvin model (Figure 5 (b)), with a retardation time (λ_{ret}). The Kelvin-Voigt model will stop deforming over time if the applied stress is not removed. The material will then flow in a viscous way with zero shear viscosity (η_0) (Figure 5(c)) until the applied stress is removed.
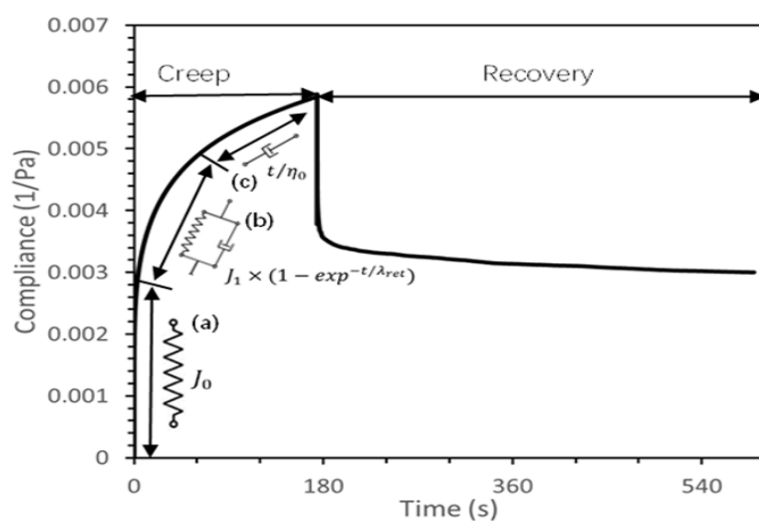
Figure 5. The creep and recovery curves of the 6I04X sample: (a) the Hookean spring, (b) the Kelvin–Voigt model, (c) the Newtonian dashpot.
Note: Augusto et al. (2013).

The creep curves of the inks (Figure 6, $0 \leqslant t \leqslant 180$ s) agree well with the Burgers model ($R^2 > 0.86$). XG, inulin and their interaction effects significantly affected this parameter ($P < 0.05$). As seen in Table 3, the control samples had the highest J_0 values and exhibited maximum compliance and elastic deformation under applied stress (Figure 6). J_0 is related to the changes in lengths and angles of chemical bonds in the material under stress, and a lower J_0 value indicates higher elasticity and deformation resistance (Laguna, Vallons, Jurgens, & Sanz, 2013; Onyango, Mutungi, Unbehend, & Lindhauer, 2010). Adding 0.4% of XG to the ink formulation (10I04X and 14I04X) did not reduce the J_0 value ($P > 0.05$). However, with higher XG amounts (0.8% and 1.2%) in the inks (6I08X, 6I12X, 10I08X, 10I12X, 14I08X, and 14I12X), J_0 values were significantly reduced ($P < 0.05$). 6I12X and 10I12X had the lowest J_0 values and exhibited the lowest compliance and elastic deformation (Figure 6). These results showed that XG improved the deformation resistance of the inks, but more XG (0.8% and 1.2%) was needed to improve the deformation resistance in the inks with 10% and 14% of inulin. XG strengthened the ink structure more than inulin despite being added in smaller amounts. The rigid structures of the XG molecule effectively resist deformation under applied stress (Imeson, 2010a). Additionally, 14I08X and 14I12X had significantly higher J_0 values ($P < 0.05$) than 6I08X and 6I12X, indicating that a high amount of inulin (14%) weakened ink deformation resistance. The connection between the particle gels formed by microcrystals of inulin dissolved in water is very fragile and can be broken under minor stress, causing a more extensive deformation (Bot, Erle, Vreeker, & Agterof, 2004; Hager et al., 2011; Kaur & Gupta, 2002). The retardation compliance (J_1) value is related to the conformational change of the molecular chain under applied stress (Onyango, Mutungi, Unbehend, & Lindhauer, 2009) and showed a similar trend to that of J_0. The control sample and 14I04X exhibited the highest J_1 values, whereas other XG-added inks had significantly lower values ($P < 0.05$), implying that XG enhances the ink's internal structure, making the molecular chain conformation difficult to change under applied stress. Also, the ink containing 14% inulin had a higher J_1 value ($P < 0.05$) and greater deformation than other inks with inulin and XG (Figure 6). Juszczak et al. (2012) found that adding 8−12% inulin increased the instantaneous and retardation deformation of corn-potato dough. J_1 was the only parameter insignificantly affected by the inulin and XG interaction effect.
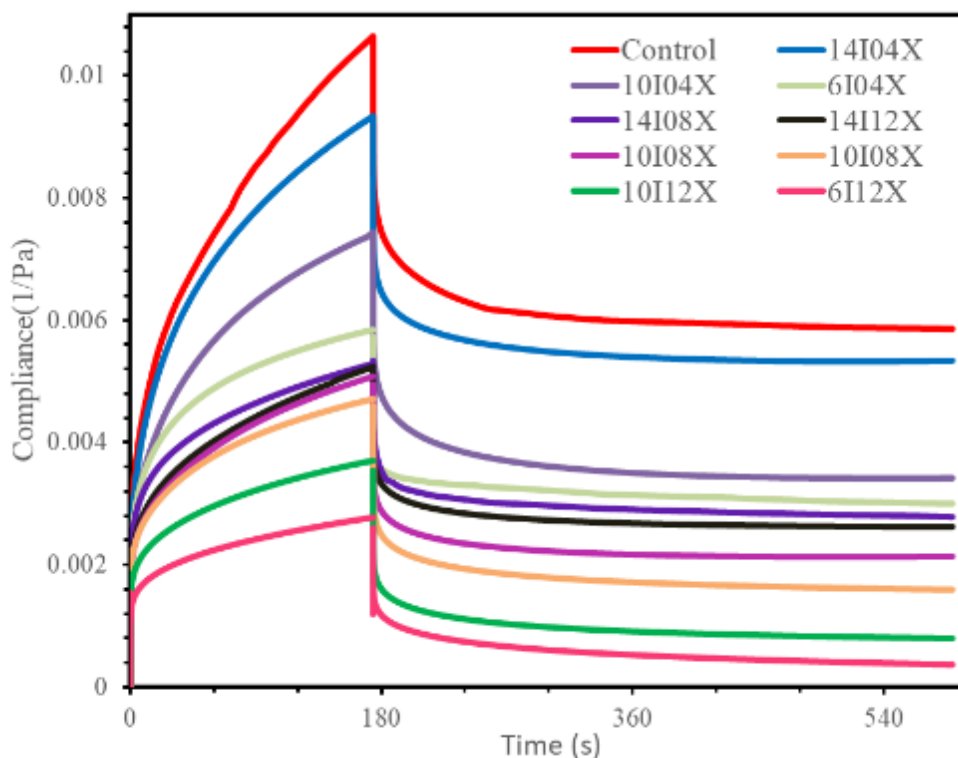

**Figure 6.** The creep and recovery curves of each ink formulation.

Table 3. The parameters of each ink formulation in the Burgers model.

Formulation	Instantaneous compliance $\times 10^{-4}(J_0, \text{Pa}^{-1})$	Retardation compliance $\times 10^{-4}(J_1, \text{Pa}^{-1})$	Retardation time $(\lambda_{ret}, \text{s})$	Zero shear viscosity $\times 10^{4}(\eta_0, \text{Pa·s})$
Control	21.82 ± 2.16^a	28.40 ± 1.65^a	6.28 ± 0.67^{ab}	2.85 ± 0.3^g
6I04X	17.73 ± 0.57^b	16.7 ± 0.86^c	3.27 ± 0.43^b	5.41 ± 0.33^e
6I08X	13.35 ± 2.13^c	11.35 ± 1.25^d	2.51 ± 0.76^c	8.58 ± 0.47^c
6I12X	8.47 ± 1.66^d	6.69 ± 0.83^e	2.43 ± 0.53^c	10.83 ± 0.24^a
10I04X	18.53 ± 1.19^{ab}	21.59 ± 2.35^b	4.82 ± 0.86^b	3.88 ± 0.28^f
10I08X	14.84 ± 1.16^{bc}	14.40 ± 0.86^{cd}	2.46 ± 0.01^c	7.27 ± 0.60^d
10I12X	10.88 ± 1.37^{cd}	9.73 ± 0.87^{de}	2.34 ± 0.19^c	9.63 ± 0.16^b
14I04X	19.69 ± 0.67^{ab}	30.9 ± 1.83^a	7.39 ± 0.44^a	3.36 ± 0.18^{fg}
14I08X	17.27 ± 0.50^b	23.63 ± 1.60^b	6.44 ± 0.65^a	4.94 ± 0.34^e
14I12X	16.33 ± 0.47^{bc}	20.16 ± 0.64^{bc}	4.37 ± 0.38^b	6.52 ± 0.40^d
One-way ANOVA – p	< 0.001	< 0.001	< 0.001	< 0.001
Two-way ANOVA – p				
Factor I (Inulin)	< 0.001	< 0.001	< 0.001	< 0.001
Factor II (XG)	< 0.001	< 0.001	< 0.001	< 0.001
Factor I × factor II	0.014	0.631	0.004	< 0.001

Note: Each formulation was tested at 25 ℃ and expressed as mean ± SD (n = 3). The lowercase letters (a, b, c, d, e, f, g) in the same column indicate significant differences at a level of confidence of 0.05.

A Two-way ANOVA showed that XG, inulin, and their interaction effects significantly impacted retardation time (λ_{ret}). Adding 0.8% and 1.2% of XG to inks with 6% and 10% of inulin (6I08X, 6I12X, 10I08X, and 10I12X) resulted in lower λ_{ret} values (P < 0.05), while other inks with inulin and XG showed higher λ_{ret} values that were not significantly different from the control. This indicates the inks with stronger internal structures (low J_0 and J_1) also exhibit shorter retardation times during deformation. Brito-Oliveira et al. (2022) found that soy protein isolates with 0.1% XG had a shorter retardation time than control samples due to material structure reinforcement by XG. Zero shear viscosity (η_0) indicates the viscosity of a material at rest. XG, inulin, and their interactions also significantly affected the value of η_0. The lowest values of η_0 were observed for the control sample and 14I04X, while 6I12X showed the highest η_0 value. This was consistent with the results obtained by the apparent viscosity in steady-state shear (Sections 3.1.2).

Once the applied stress is removed (Figure 6, recovery phase: 180 ≤ t ≤ 600 s), the ability of the ink to regain its structure is called "elastic recovery" (Pulatsu et al., 2020). The recovery rate calculated according to Equation 4 is shown in Figure 7. XG, inulin and their interactions significantly affected this parameter (P < 0.05). Lower recovery rates were seen in control samples and inks with 0.4% of XG (P > 0.05, 6I04X, 10I04X, and 14I04X). A higher amount of XG (0.8% and 1.2%) added to the inks (6I08X, 6I12X, 10I08X, and 10I12X) resulted in a significant increase in the recovery rate (P < 0.05). This suggests that these inks have strong structural recoverability and thus exhibit less permanent deformation. Xing et al. (2022) also found that the black fungus pastes with 0.6% XG showed a higher elastic recovery rate than the control sample. The complex network structure of the XG molecular stores energy during creep and releases it after stress is removed, improving the ink recovery rate (Xing et al., 2022). As the inulin amount increased from 6% to 10%, the recovery rate for 6I08X, 10I08X, 6I12X, and 10I12X decreased (P < 0.05) but remained higher than the control sample (P < 0.05). Inks with 14% inulin (14I04X, 14I08X, and 14I12X) had the greatest recovery rate decrease and were not significantly different (P > 0.05) from the control sample. Inulin weakened the inks' internal structure, making them more susceptible to damage from applied stress and lowering recovery rates. This property may not be conducive to maintaining shape in the printed product.
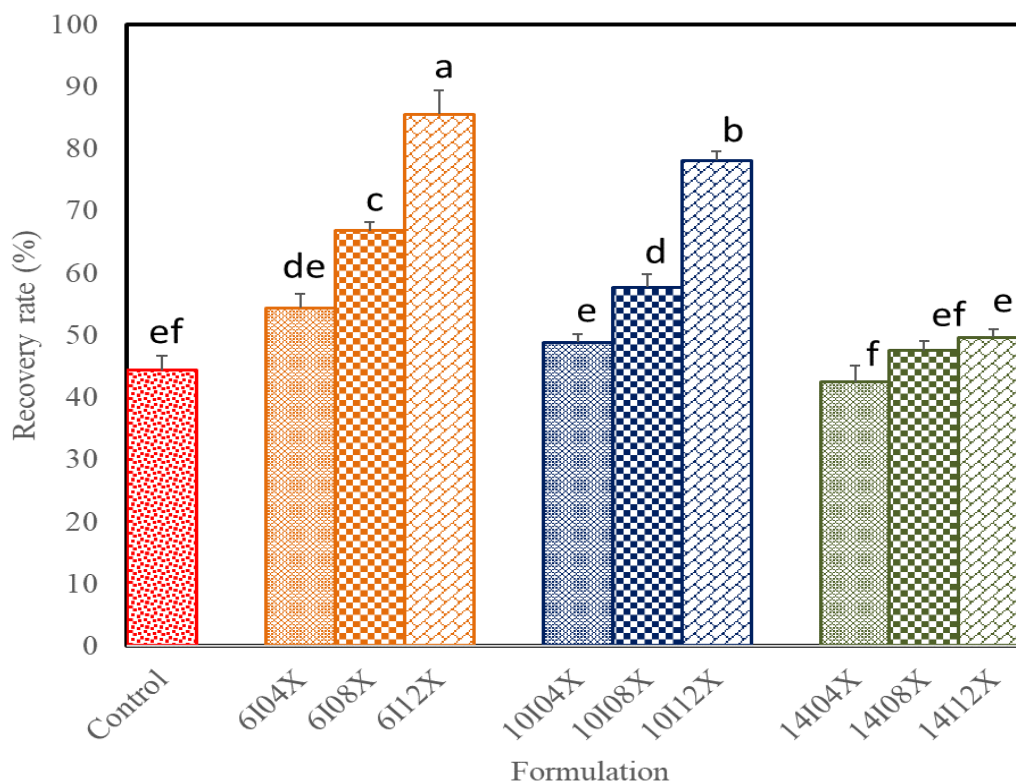
Figure 7. The recovery rate of each ink formulation. The lowercase letters (a, b, c, d, e, f, g) in the histogram indicate significant differences at a level of confidence of 0.05.
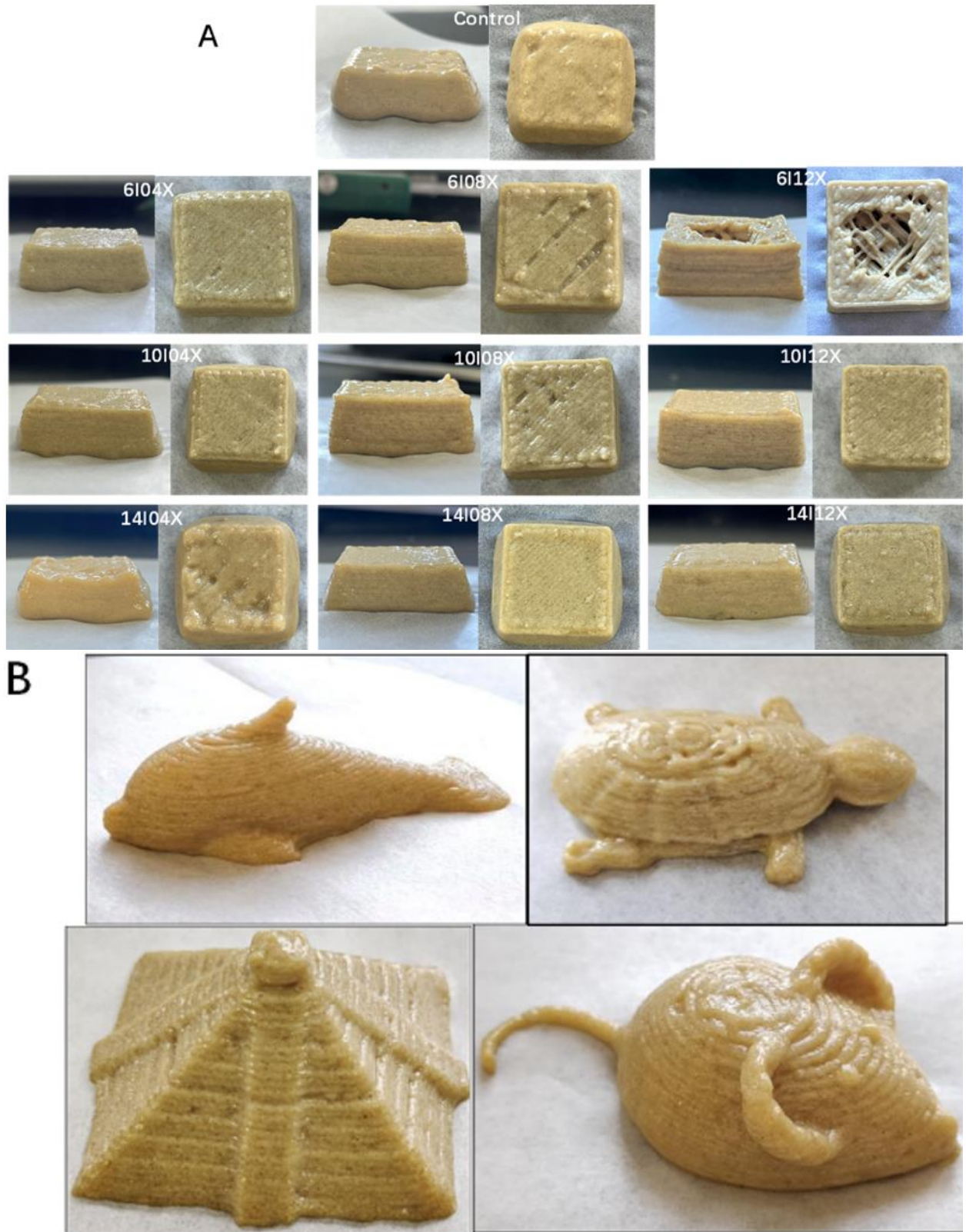
3.2. 3D Printed Structures

The structural difference in the 3D printed products was evaluated by examining the 3D cuboids (Figure 8). The control samples, 0.4% XG samples (6I04X, 10I04X, and 14I04X), and 14% inulin samples (14I08X and 14I12X) deformed variously.

A trapezoidal collapse structure is observed on the sides of the printed samples. These samples lacked sufficient mechanical strength (low yield stress and G') and deformation resistance (high J_0 and J_1) to support the deposited layer and poor recoverability after deformation, causing 3D printed shapes to collapse under gravity. After adding 0.8% and 1.2% of XG, the 3D-printed products (6I08X, 6I12X, 10I08X, and 10I12X) deformed less and were close to the design model.

A high amount of XG (0.8% and 1.2%) strengthened the ink (discussed in 3.1), making it better at supporting the 3D printed structure (Costakis, Rueschhoff, Diaz-Cano, Youngblood, & Trice, 2016; Liu, Bhandari, et al., 2020). Although the 6I12X sample was a cuboid, it had significant layering on the sides and breaks and voids at the top. The high viscosity of this sample (highest K value) caused low ink fluidity, which prevented continuous extrusion during the printing, causing thread breakage.

Kim et al. (2019) found that a large amount of XG (1 and 2 g/100g) reduced the fluidity of cookie dough, resulting in poor resolution at the top of the model structure. After adding a suitable amount of inulin and XG, 10I12X was the best 3D-printed cuboid with a fine and smooth surface texture. The 10I12X-printed other shapes were also observed to have a delicate appearance with acceptable and perfect layers (Figure 8B).

Figure 8. The photographs of the varying formulations of 3D printed Tartary buckwheat paste: (A) side view (left) and top view (right) of 3D printed cuboids and (B) various shapes 3D printed using the 10I12X ink formulation.

3.3. Microstructural Analysis

Figure 9 depicts the microstructure of the ink as seen by scanning electron microscopy (SEM). The control sample and samples with 0.4% of XG (6I04X, 10I04X, and 14I04X) had structures with many micropores (circled red) in the material. Such arrangements might weaken the mechanical strength of the inks, and the 3D-printed

structure might collapse (Figure 8A). Liu, Zhang, and Bhandari (2018) reported that the porous microstructure and uneven pore distribution in mashed potato ink changed the extrudability and structural stability of 3D-printed products. The non-porous, continuous, and compact structure could be seen in the samples with 0.8% and 1.2% of XG (6I08X, 6I12X, 10I08X, and 10I12X). This structure could maintain the printed shape, as the best 3D printed shape was found in 10I12X (Figure 8A). Kim et al. (2019) also observed non-porous microstructures in cookie dough with 0.5 g/100g of added XG, which showed strong deformation resistance. However, some micropores similar to those in the control sample were observed in the inks containing 14% inulin (14I08X and 14I12X). This result confirmed the undesirable effect of higher inulin on the ink's structure, which weakened its mechanical stability (discussed in Sections 3.1.1 and 3.1.3).
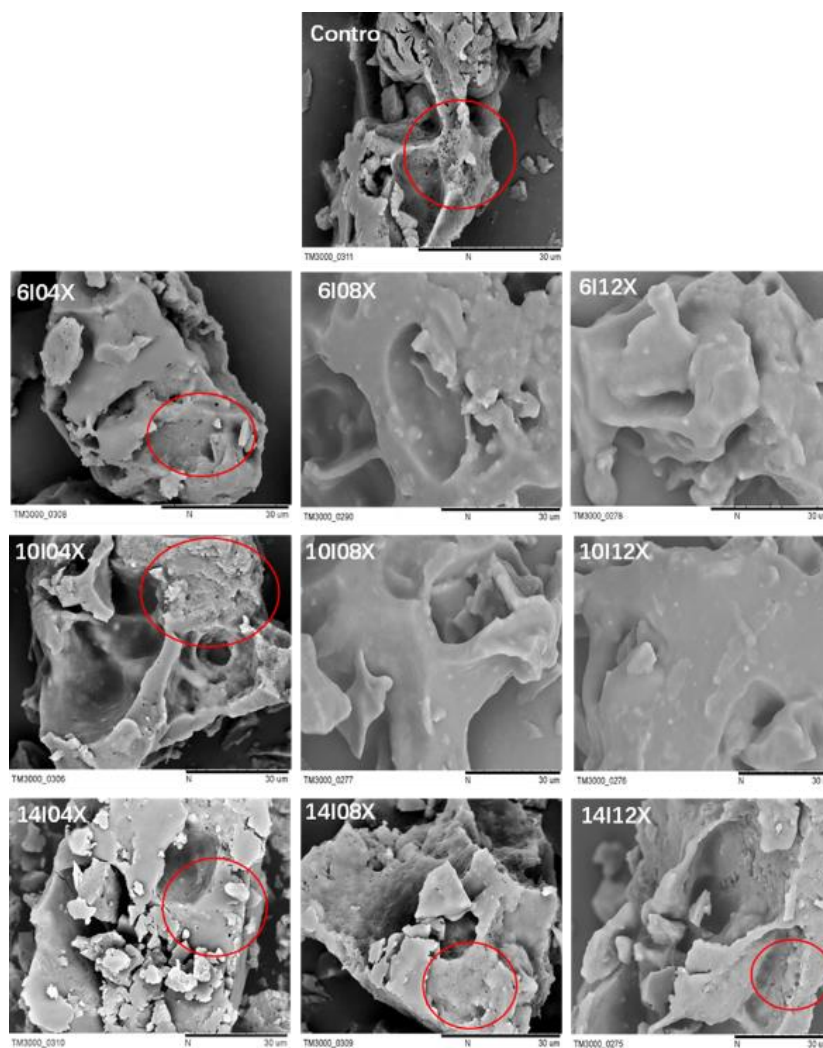
Figure 9. The scanning electron microscopy (SEM) images of the ink. at a scale bar of 30 μm and 2000×magnification.

4. CONCLUSION

It was found that the amount of XG and inulin significantly affected the rheology of Tartary buckwheat paste. A low amount of XG (0.4%) did not change these rheological properties, but a high amount (0.8% and 1.2%) increased the ink's viscoelasticity and shifted it towards solid-like with high consistency. It required more extrusion force to start flowing, reducing ink printability. However, a high amount of inulin (10% and 14%) shifted the ink to liquid-like with a low consistency. Two-way ANOVA demonstrated that the interaction effect of XG and inulin diluted the ink and improved its fluidity, giving it good printability. Meanwhile, this study identified that 10I12X ink with 10% inulin and 1.2% XG was the best combination for 3D printing. This ink showed high deformation resistance and

recoverability in creep recovery tests, and its SEM indicated a non-porous, compact structure. These properties gave the ink a good self-supporting ability to obtain the best 3D-printed shape. Although this study identified the most suitable amount of inulin and XG in Tartary buckwheat paste that can be used for 3D printing, the texture, sensory, and overall acceptability of the printed products are unclear and require further study.

REFERENCES

Abdel-Aal, E. S. M., Rabalski, I., Hernandez, M., L'Hocine, L., Patterson, C. A., & Hucl, P. (2019). Effect of sodium chloride, sucrose, and xanthan gum on pasting properties and gel syneresis of hairless canary seed starch. *Cereal Chemistry, 96*(5), 908-919. https://doi.org/10.1002/cche.10194

Augusto, P. E., Ibarz, A., & Cristianini, M. (2013). Effect of high pressure homogenization (HPH) on the rheological properties of tomato juice: Creep and recovery behaviours. *Food Research International, 54*(1), 169-176. https://doi.org/10.1016/j.foodres.2013.06.027

Bot, A., Erle, U., Vreeker, R., & Agterof, W. G. (2004). Influence of crystallisation conditions on the large deformation rheology of inulin gels. *Food Hydrocolloids, 18*(4), 547-556. https://doi.org/10.1016/j.foodhyd.2003.09.003

Brito-Oliveira, T. C., Moraes, I. C., Pinho, S. C., & Campanella, O. H. (2022). Modeling creep/recovery behavior of cold-set gels using different approaches. *Food Hydrocolloids, 123*, 107183. https://doi.org/10.1016/j.foodhyd.2021.107183

Chang, Y., Lim, S., & Yoo, B. (2004). Dynamic rheology of corn starch–sugar composites. *Journal of Food Engineering, 64*(4), 521-527. https://doi.org/10.1016/j.jfoodeng.2003.08.017

Chiavaro, E., Vittadini, E., & Corradini, C. (2007). Physicochemical characterization and stability of inulin gels. *European Food Research and Technology, 225*, 85-94. https://doi.org/10.1007/s00217-006-0385-y

Costakis, J. W. J., Rueschhoff, L. M., Diaz-Cano, A. I., Youngblood, J. P., & Trice, R. W. (2016). Additive manufacturing of boron carbide via continuous filament direct ink writing of aqueous ceramic suspensions. *Journal of the European Ceramic Society, 36*(14), 3249-3256. https://doi.org/10.1016/j.jeurceramsoc.2016.06.002

Coxam, V. (2005). Inulin-type fructans and bone health: State of the art and perspectives in the management of osteoporosis. *British Journal of Nutrition, 93*(S1), S111-S123. https://doi.org/10.1079/bjn20041341

De Gennaro, S., Birch, G. G., Parke, S. A., & Stancher, B. (2000). Studies on the physicochemical properties of inulin and inulin oligomers. *Food Chemistry, 68*(2), 179-183. https://doi.org/10.1016/s0308-8146(99)00173-9

Demirkesen, I., Mert, B., Sumnu, G., & Sahin, S. (2010). Rheological properties of gluten-free bread formulations. *Journal of Food Engineering, 96*(2), 295-303. https://doi.org/10.1016/j.jfoodeng.2009.08.004

Godoi, F. C., Prakash, S., & Bhandari, B. R. (2016). 3d printing technologies applied for food design: Status and prospects. *Journal of Food Engineering, 179*, 44-54. https://doi.org/10.1016/j.jfoodeng.2016.01.025

Guggisberg, D., Cuthbert-Steven, J., Piccinali, P., Bütikofer, U., & Eberhard, P. (2009). Rheological, microstructural and sensory characterization of low-fat and whole milk set yoghurt as influenced by inulin addition. *International Dairy Journal, 19*(2), 107-115. https://doi.org/10.1016/j.idairyj.2008.07.009

Hager, A.-S., Ryan, L. A., Schwab, C., Gänzle, M. G., O'Doherty, J. V., & Arendt, E. K. (2011). Influence of the soluble fibres inulin and oat β-glucan on quality of dough and bread. *European Food Research and Technology, 232*, 405-413. https://doi.org/10.1007/s00217-010-1409-1

Imeson, A. (2010a). Food stabilisers, thickeners and gelling agents. In Graham, S (Eds.), Xanthan Gum. In (pp. 325-339): Blackwell Publishing Ltd. https://doi.org/10.1002/9781444314724.

Imeson, A. (2010b). Food stabilisers, thickeners and gelling agents. In Rudy, W (Eds.), Inulin. In (pp. 180-194): Blackwell Publishing Ltd. https://doi.org/10.1002/9781444314724.

Ji, X., Yin, M., Hao, L., Shi, M., Liu, H., & Liu, Y. (2021). Effect of inulin on pasting, thermal, rheological properties and in vitro digestibility of pea starch gel. *International Journal of Biological Macromolecules, 193*, 1669-1675. https://doi.org/10.1016/j.ijbiomac.2021.11.004

Jiménez, M., Romero, L., Domínguez, I. A., Espinosa, M. D. M., & Domínguez, M. (2019). Additive manufacturing technologies: An overview about 3D printing methods and future prospects. *Complexity, 2019.* https://doi.org/10.1155/2019/9656938

Juszczak, L., Witczak, T., Ziobro, R., Korus, J., Cieślik, E., & Witczak, M. (2012). Effect of inulin on rheological and thermal properties of gluten-free dough. *Carbohydrate Polymers, 90*(1), 353-360. https://doi.org/10.1016/j.carbpol.2012.04.071

Kaur, N., & Gupta, A. K. (2002). Applications of inulin and oligofructose in health and nutrition. *Journal of Biosciences, 27*, 703-714. https://doi.org/10.1007/bf02708379

Kim, H. W., Lee, I. J., Park, S. M., Lee, J. H., Nguyen, M.-H., & Park, H. J. (2019). Effect of hydrocolloid addition on dimensional stability in post-processing of 3D printable cookie dough. *LWT-, Food Science and Technology, 101*, 69-75. https://doi.org/10.1016/j.lwt.2018.11.019

Kou, X., Luo, D., Li, Y., Xu, B., Zhang, K., Li, P., . . . Liu, J. (2018). Effect of inulin with different degree of polymerisation on textural and rheological properties of wheat starch–effect of inulin on gel properties of starch. *International Journal of Food Science & Technology, 53*(11), 2576-2585. https://doi.org/10.1111/ijfs.13852

Laguna, L., Vallons, K. J., Jurgens, A., & Sanz, T. (2013). Understanding the effect of sugar and sugar replacement in short dough biscuits. *Food and Bioprocess Technology, 6*, 3143-3154. https://doi.org/10.1007/s11947-012-0968-5

Liu, Y., Liang, X., Saeed, A., Lan, W., & Qin, W. (2019). Properties of 3D printed dough and optimization of printing parameters. *Innovative Food Science & Emerging Technologies, 54*, 9-18. https://doi.org/10.1016/j.ifset.2019.03.008

Liu, Z., Bhandari, B., & Zhang, M. (2020). Incorporation of probiotics (Bifidobacterium animalis subsp. Lactis) into 3D printed mashed potatoes: Effects of variables on the viability. *Food Research International, 128*, 108795. https://doi.org/10.1016/j.foodres.2019.108795

Liu, Z., Zhang, M., & Bhandari, B. (2018). Effect of gums on the rheological, microstructural and extrusion printing characteristics of mashed potatoes. *International Journal of Biological Macromolecules, 117*, 1179-1187. https://doi.org/10.1016/j.ijbiomac.2018.06.048

Liu, Z., Zhang, M., Bhandari, B., & Wang, Y. (2017). 3D printing: Printing precision and application in food sector. *Trends in Food Science & Technology, 69*, 83-94. https://doi.org/10.1016/j.tifs.2017.08.018

Liu, Z., Zhang, M., & Ye, Y. (2020). Indirect prediction of 3D printability of mashed potatoes based on LF-NMR measurements. *Journal of Food Engineering, 287*, 110137. https://doi.org/10.1016/j.jfoodeng.2020.110137

Luo, D., Liang, X., Xu, B., Kou, X., Li, P., Han, S., . . . Zhou, L. (2017). Effect of inulin with different degree of polymerization on plain wheat dough rheology and the quality of steamed bread. *Journal of Cereal Science, 75*, 205-212. https://doi.org/10.1016/j.jcs.2017.04.009

Mieszkowska, A., & Marzec, A. (2016). Effect of polydextrose and inulin on texture and consumer preference of short-dough biscuits with chickpea flour. *LWT- Food Science and Technology, 73*, 60-66. https://doi.org/10.1016/j.lwt.2016.05.036

Onyango, C., Mutungi, C., Unbehend, G., & Lindhauer, M. G. (2009). Creep-recovery parameters of gluten-free batter and crumb properties of bread prepared from pregelatinised cassava starch, sorghum and selected proteins. *International Journal of Food Science & Technology, 44*(12), 2493-2499. https://doi.org/10.1111/j.1365-2621.2009.02048.x

Onyango, C., Mutungi, C., Unbehend, G., & Lindhauer, M. G. (2010). Rheological and baking characteristics of batter and bread prepared from pregelatinised cassava starch and sorghum and modified using microbial transglutaminase. *Journal of Food Engineering, 97*(4), 465-470. https://doi.org/10.1016/j.jfoodeng.2009.11.002

Peressini, D., & Sensidoni, A. (2009). Effect of soluble dietary fibre addition on rheological and breadmaking properties of wheat doughs. *Journal of Cereal Science, 49*(2), 190-201. https://doi.org/10.1016/j.jcs.2008.09.007

Pulatsu, E., Su, J.-W., Lin, J., & Lin, M. (2020). Factors affecting 3D printing and post-processing capacity of cookie dough. *Innovative Food Science & Emerging Technologies, 61*, 102316. https://doi.org/10.1016/j.ifset.2020.102316

Roberfroid, M. (2004). *Inulin-type fructans: Functional food ingredients* (1st ed.). Boca Raton: CRC Press. https://doi.org/10.1201/9780203504932.

Rong, L., Shen, M., Wen, H., Xiao, W., Li, J., & Xie, J. (2022). Effects of xanthan, guar and Mesona chinensis Benth gums on the pasting, rheological, texture properties and microstructure of pea starch gels. *Food Hydrocolloids, 125*, 107391. https://doi.org/10.1016/j.foodhyd.2021.107391

Shalviri, A., Liu, Q., Abdekhodaie, M. J., & Wu, X. Y. (2010). Novel modified starch–xanthan gum hydrogels for controlled drug delivery: Synthesis and characterization. *Carbohydrate Polymers, 79*(4), 898-907. https://doi.org/10.1016/j.carbpol.2009.10.016

Shoaib, M., Shehzad, A., Omar, M., Rakha, A., Raza, H., Sharif, H. R., . . . Niazi, S. (2016). Inulin: Properties, health benefits and food applications. *Carbohydrate Polymers, 147*, 444-454. https://doi.org/10.1016/j.carbpol.2016.04.020

Sinkovič, L., Deželak, M., & Meglič, V. (2022). Macro/microelements, nutrients and bioactive components in common and Tartary buckwheat (Fagopyrum spp.) grain and stone-milling fractions. *LWT, 161*, 113422. https://doi.org/10.1016/j.lwt.2022.113422

Sinkovič, L., Sinkovič, D. K., & Meglič, V. (2021). Milling fractions composition of common (Fagopyrum esculentum Moench) and Tartary (Fagopyrum tataricum (L.) Gaertn.) buckwheat. *Food Chemistry, 365*, 130459. https://doi.org/10.1016/j.foodchem.2021.130459

Tárrega, A., Torres, J., & Costell, E. (2011). Influence of the chain-length distribution of inulin on the rheology and microstructure of prebiotic dairy desserts. *Journal of Food Engineering, 104*(3), 356-363. https://doi.org/10.1016/j.jfoodeng.2010.12.028

Torres, J. D., Tárrega, A., & Costell, E. (2010). Storage stability of starch-based dairy desserts containing long-chain inulin: Rheology and particle size distribution. *International Dairy Journal, 20*(1), 46-52. https://doi.org/10.1016/j.idairyj.2009.08.001

Tsai, H., Deng, H., Tsai, S., & Hsu, Y. (2012). Bioactivity comparison of extracts from various parts of common and tartary buckwheats: Evaluation of the antioxidant-and angiotensin-converting enzyme inhibitory activities. *Chemistry Central Journal, 6*(1), 1-5. https://doi.org/10.1186/1752-153x-6-78

Witczak, T., Witczak, M., & Ziobro, R. (2014). Effect of inulin and pectin on rheological and thermal properties of potato starch paste and gel. *Journal of Food Engineering, 124*, 72-79. https://doi.org/10.1016/j.jfoodeng.2013.10.005

Xing, X., Chitrakar, B., Hati, S., Xie, S., Li, H., Li, C., . . . Mo, H. (2022). Development of black fungus-based 3D printed foods as dysphagia diet: Effect of gums incorporation. *Food Hydrocolloids, 123*, 107173. https://doi.org/10.1016/j.foodhyd.2021.107173

Yao, Y., Shan, F., Bian, J., Chen, F., Wang, M., & Ren, G. (2008). D-chiro-inositol-enriched tartary buckwheat bran extract lowers the blood glucose level in KK-Ay mice. *Journal of Agricultural and Food Chemistry, 56*(21), 10027-10031. https://doi.org/10.1021/jf801879m

Zhang, R., Yao, Y., Wang, Y., & Ren, G. (2011). Antidiabetic activity of isoquercetin in diabetic KK-A y mice. *Nutrition & Metabolism, 8*, 1-6. https://doi.org/10.1186/1743-7075-8-85